**Journal of Neonatal Surgery**
***ISSN(Online): 2226-0439***
***Vol. 14, Issue 4s (2025)***
*https://www.jneonatalsurg.com*

OPEN ACCESS

# Chronotherapeutic Circadian-Based Pulsatile Drug Delivery of Etodolac for Morning Stiffness in Rheumatoid Arthritis

**Vaibhav P. Uplanchiwar[1], Koushik Narayan Sarma[2], Tabrej Mujawar[3*], V. Mythily[4], Perli.Kranti Kumar[5], Parameswari Prabhu[6], Touseef Begum[7], Swetha.M[8]**

[1]Nagpur College of Pharmacy, Wanadongri, Hingna Road, Nagpur-441110, Maharashtra Pin- 441110.
[2]Faculty of Pharmaceutical Science, Assam down town University, Panikhaiti, Guwahati, Assam India Pin-781026.
[3]Department of Pharmacology, Gangamai College of Pharmacy, Nagaon Dhule MS India Pin- 424005.
[4]Department of Biomedical Engineering, Jerusalem College of Engineering, Narayanapuram, Pallikaranai, Chennai. Pin- 600100.
[5]Department of Pharmaceutical Analysis, School of Pharmaceutical Sciences, Sandip University, Nashik, Maharashtra 422213.
[6]Department of Pharmaceutics Mohammed Sathak AJ College of Pharmacy Medavakkam Road, Sholinganallur, Chennai, Tamil Nadu Pin-600119.
[7]Department of Pharmaceutical Sciences, Ibn Sina National College for Medical Studies, P.O. Box 31906, Jeddah 21418, Kingdom of Saudi Arabia.
[8]Department of Pharmaceutics, PERI college of Pharmacy, Mannivakkam, Chennai , India Pin- 600048.
[*]**Corresponding author**
Tabrej Mujawar
Department of Pharmacology, Gangamai College of Pharmacy, Nagaon Dhule MS India Pin- 424005.
Email ID: tabrejpharma@gmail.com

.Cite this paper as: Vaibhav P. Uplanchiwar, Koushik Narayan Sarma, Tabrej Mujawar, V. Mythily, Perli.Kranti Kumar, Parameswari Prabhu, Touseef Begum, Swetha.M,(2025)Chronotherapeutic Circadian-Based Pulsatile Drug Delivery of Etodolac for Morning Stiffness in Rheumatoid Arthritis. *Journal of Neonatal Surgery*, 14(4s), 833-848.

**ABSTRACT**
This study focuses on the development of chronomodulated delivery systems for Etodolac, aimed at optimizing therapeutic outcomes in rheumatoid arthritis management. Core and coated microparticles were formulated using chitosan and Eudragit polymers, employing varying drug-to-polymer ratios and stirring speeds to achieve precise release profiles. Scanning electron microscopy confirmed the uniformity and integrity of the microparticles, with particle sizes ranging from 20.52 ± 0.79 µm to 105.45 ± 6.74 µm. Encapsulation efficiencies reached up to 98.34 ± 0.09% in coated formulations, demonstrating enhanced drug retention. Drug release studies revealed that coated microparticles followed controlled and sustained release patterns, aligning with zero-order and Higuchi kinetics, suitable for chronomodulated delivery. FTIR analysis confirmed chemical compatibility between Etodolac and excipients, ensuring formulation stability. The findings indicate that optimized formulation parameters, including drug-to-polymer ratios, stirring speeds, and polymer coatings, enabled effective delivery aligned with rheumatoid arthritis chronotherapy, targeting peak symptoms in early morning hours. This study highlights the potential of Etodolac microparticles for tailored drug delivery, improving patient compliance and therapeutic efficacy in managing rheumatoid arthritis.

***Keywords:*** *Etodolac, Chronotherapeutic, Chronomodulated, Microparticle, Eudragit, Chitosan, pH Dependent.*

## 1. INTRODUCTION

Rheumatoid arthritis (RA) is a chronic autoimmune disorder characterized by inflammation, pain, and stiffness in the joints, often leading to progressive joint damage and disability. The disease affects millions of individuals worldwide, with symptoms following a distinct circadian rhythm. Studies have shown that RA symptoms, including joint stiffness and pain, are most pronounced in the early morning hours, largely due to fluctuations in pro-inflammatory cytokines and cortisol levels (Radu and Bungau, 2021, Huang et al., 2021, Smolen et al., 2016). Traditional pharmacological treatments, including non-steroidal anti-inflammatory drugs (NSAIDs) like

Etodolac, are often effective in alleviating symptoms. However, their therapeutic efficacy can be further enhanced by aligning drug delivery with the circadian patterns of RA symptoms, a concept known as chronotherapy (Zvaifler, 1989).

Chronotherapy emphasizes delivering drugs at optimal times to maximize therapeutic outcomes while minimizing adverse effects. This approach is particularly relevant for RA, as it ensures peak drug release coincides with the onset of symptoms. Controlled-release drug delivery systems have gained prominence in achieving this goal, offering sustained or delayed drug release tailored to the disease's circadian rhythm (Wasserman, 2011, McInnes and Schett, 2011, Ngian, 2010). Microparticles have emerged as a promising platform for chronomodulated delivery, owing to their ability to encapsulate drugs efficiently, protect them from premature degradation, and release them in a controlled manner (Roy and Shahiwala, 2009, Kikuchi et al., 1999, Patel and Patel, 2009, Wilding et al., 1994).

Etodolac, a selective cyclooxygenase-2 (COX-2) inhibitor, has proven effective in managing inflammation and pain associated with RA. However, conventional formulations may not align with the disease's circadian rhythm, resulting in suboptimal symptom control and potential side effects due to unregulated drug release (Balfour and Buckley, 1991, Pena, 1990). The development of a microparticulate system incorporating chronomodulated principles offers an innovative solution to this challenge. Using polymers such as chitosan and Eudragit, these systems can be designed to achieve controlled release, ensuring targeted drug delivery to coincide with peak RA symptom severity (Aodah, 2009, Smolensky et al., 2007, Warwick, 1988, Cochrane and Clark, 1975, Balfour and Buckley, 1991, Pena, 1990).

This study focuses on the formulation, characterization, and evaluation of Etodolac-loaded microparticles designed for chronomodulated delivery in RA management. Chitosan, a biocompatible and biodegradable polymer, was employed as the core matrix material, while Eudragit coatings were used to achieve pH-sensitive and delayed release properties. Various drug-to-polymer ratios, stirring speeds, and coating conditions were optimized to produce microparticles with high encapsulation efficiency, uniform size distribution, and tailored release profiles (Soni et al., 2011, Roy and Shahiwala, 2009, Kikuchi and Okano, 2002, Bogin and Ballard, 1992).

The prepared formulations were subjected to rigorous evaluation, including particle size analysis, encapsulation efficiency, in vitro drug release studies, and Fourier Transform Infrared (FTIR) spectroscopy to assess drug-polymer compatibility. Scanning electron microscopy was used to analyze the morphological characteristics of the microparticles, confirming the uniformity and integrity of the core and coated particles. Drug release kinetics were analyzed using mathematical models such as zero-order, first-order, Higuchi, and Korsmeyer-Peppas to elucidate the underlying mechanisms. This research aims to establish a robust foundation for using Etodolac-loaded microparticles in chronotherapy, providing an effective strategy for managing RA symptoms while improving patient compliance. The findings contribute to advancing drug delivery systems tailored to meet the specific needs of chronic inflammatory diseases, emphasizing the importance of aligning therapeutic interventions with the body’s circadian rhythms.

## 2. MATERIALS AND METHODS

### Drugs, chemicals and reagents

Etodolac sulfate, the key drug used in the study, was generously provided as a gift sample by Cygnus Pharma, located in Baddi, Himachal Pradesh, India. The polymer Chitosan (CS), known for its biocompatibility and biodegradability, was obtained from Himedia, India, ensuring high-quality raw material for the formulation process. Eudragit L 100 and S 100, both extensively used in pH-sensitive drug delivery systems, were sourced from Loba Chemicals, Mumbai, India, which specializes in high-grade pharmaceutical excipients. Light paraffin oil and glutaraldehyde (GA), essential for microparticle preparation and cross-linking, respectively, were purchased from Sigma Aldrich, Mumbai, India, ensuring the use of reliable and standardized reagents. Additionally, Span 80, a critical emulsifier for stabilizing formulations, along with acetone and petroleum ether, essential solvents for various processing steps, were also procured from Sigma Aldrich, Mumbai, India. The selection of these high-quality materials from reputable suppliers underscores the meticulous approach adopted in this research to ensure consistency and reproducibility in the formulation and evaluation of Etodolac-loaded microparticles.

### Preparation of Core microparticle

Etodolac-loaded microparticles were prepared using the emulsion cross-linking method with formulations as detailed in Table 1. The process involved dissolving Chitosan in a 1% acetic acid solution to form the aqueous phase. The drug, Etodolac sulfate, was added to the Chitosan solution in the specified drug-to-polymer ratios (as per Table 1) under constant stirring to achieve a uniform dispersion. The emulsification process was carried out by slowly adding the aqueous phase into the continuous phase, which consisted of light paraffin oil containing Span-80 as a surfactant. The concentration of Span-80 was varied according to Table 1 to stabilize the emulsified droplets. The mixture was subjected to continuous stirring at the designated stirring speeds using a

mechanical stirrer to form a stable water-in-oil (W/O) emulsion. The stirring speeds were optimized for each formulation, ranging from 600 to 2400 rpm, as specified. The volume of the continuous phase was maintained at 125–130 ml, and emulsification was continued for 160 minutes to ensure the formation of uniformly sized droplets. Cross-linking of the Chitosan was achieved by adding glutaraldehyde as a cross-linking agent. A fixed quantity of glutaraldehyde (3 ml) with a concentration of 2.6% w/v was added dropwise into the emulsion under stirring, facilitating the stabilization of the microparticles. After the emulsification and cross-linking processes, the formed microparticles were separated by centrifugation at 3000 rpm, followed by multiple washes with petroleum ether to remove residual oil. The microparticles were then air-dried overnight to remove traces of solvent. This systematic approach allowed the preparation of Etodolac-loaded microparticles with variations in Chitosan concentration, Span-80 levels, stirring speeds, and emulsification conditions, as outlined in Table 1, providing a robust framework for evaluating the effect of formulation variables on the characteristics of the microparticles (Umadevi et al., 2010, Gao et al., 2011, Liu et al., 2007, Dhawan et al., 2004).

**Table 1.** Formulation table showing the composition of the formulations

| Formulation Code | Chitosan Concentration (Drug to Polymer Ratio) | Span-80 Concentration (% w/v) | Stirring Speed (rpm) | Continuous Phase Volume (ml) | Emulsification Time (min) | Glutaraldehyde Quantity (ml) | Glutaraldehyde Concentration (% w/v) |
|---|---|---|---|---|---|---|---|
| CTF-1 | 1:1 | 0.6 | 600 | 130 | 160 | 3.0 | 2.6 |
| CTF-2 | 1:1 | 1.2 | 1200 | 130 | 160 | 3.0 | 2.6 |
| CTF-3 | 1:1 | 1.8 | 1800 | 130 | 160 | 3.0 | 2.6 |
| CTF-4 | 1:1 | 2.4 | 2400 | 130 | 160 | 3.0 | 2.6 |
| CTF-5 | 1:2 | 0.6 | 1500 | 125 | 160 | 3.0 | 2.6 |
| CTF-6 | 1:3 | 1.2 | 1500 | 125 | 160 | 3.0 | 2.6 |
| CTF-7 | 1:4 | 1.8 | 1500 | 125 | 160 | 3.0 | 2.6 |
| CTF-8 | 1:5 | 2.4 | 1500 | 125 | 160 | 3.0 | 2.6 |

**Coating of Chitosan (CS) Microparticles**

The coating process for the Chitosan (CS) microparticles was conducted to achieve a pH-sensitive release profile and improve stability. The procedure began by preparing a coating solution using Eudragit polymers in different ratios, as detailed in Table 1. Eudragit L 100 and S 100 were dissolved in a 10 ml organic solvent mixture of acetone and ethanol in a 2:1 ratio. This solvent combination was selected to ensure the complete dissolution of the Eudragit polymers while maintaining compatibility with the chitosan core microparticles. The optimized batch of chitosan core microparticles was dispersed into the prepared polymer solution, ensuring uniform exposure to the coating material. This dispersion was then introduced into 70 ml of liquid paraffin containing Span 80 as an emulsifier to stabilize the coating process. The mixture was subjected to high-speed stirring at 1500 rpm for 3 hours at room temperature to facilitate the evaporation of the organic solvents. The gradual removal of the solvents promoted the uniform deposition of the Eudragit polymer onto the surface of the chitosan microparticles. Once the solvent evaporation process was complete, the coated microparticles were separated from the liquid paraffin by filtration. To remove residual traces of petroleum ether and liquid paraffin, the microparticles were washed thoroughly with n-hexane. This step ensured a clean surface and minimized potential impurities. The final coated microparticles were dried in a controlled environment at 30°C for 24 hours to ensure complete removal of residual solvents and stabilize the coating. This coating process resulted in microparticles with a robust and uniform polymeric layer, enhancing their pH-sensitive properties and ensuring suitability for chronotherapeutic drug delivery applications (Umadevi et al., 2010).

**Determination of mean particle size and particle size distribution**

The mean particle size and particle size distribution of both unloaded and drug-loaded microspheres were determined using optical microscopy with a calibrated compound microscope. This method ensured precise measurement of particle dimensions, critical for evaluating the uniformity and performance of the microspheres. A small quantity of the microspheres was suspended in 10 ml of purified water to prepare the sample for analysis. The suspension was subjected to ultrasonication for 5 seconds using an ultrasonic bath to prevent particle aggregation and ensure a homogenous dispersion of the microspheres. Ultrasonication was performed carefully to avoid damage to the microspheres. A drop of the well-dispersed suspension was carefully placed onto a clean glass slide using a micropipette to prevent excess solution. The slide was gently tapped to distribute the particles evenly and was subsequently mounted on the microscope stage for observation. The Feret's diameter, a measure of the particle's apparent size based on its maximum caliper length, was determined for at least 300 particles per sample to provide statistically significant results. Measurements were carried out using a

calibrated ocular micrometer, which had been pre-verified with a standard calibration slide for accuracy. The mean particle size was calculated as the average of these measurements, and the particle size distribution was analyzed to assess the uniformity of the microspheres. This method allowed for the detailed assessment of both unloaded and drug-loaded microspheres, offering insights into the influence of formulation parameters such as polymer concentration, emulsification conditions, and cross-linking on particle size and distribution. The results were expressed as mean ± standard deviation to account for variability and ensure reliability in the findings.

**Determination of Uniformity Index**

The determination of the Uniformity Index (UI) was conducted to assess the consistency of particle size distribution within the prepared microspheres, as uniformity is a critical parameter for ensuring reproducibility and optimal formulation performance. The UI was calculated using the formula UI=D90−D10/D50, D90, D50 and D10 represent the particle sizes below which 90%, 50%, and 10% of the total particles fall, respectively. Particle size data were obtained through optical microscopy or laser diffraction, with at least 300 particles analyzed per sample to ensure statistical reliability. The percentile values were derived from the cumulative particle size distribution curve, and the formula was applied to compute the UI for each batch of microspheres. A lower UI value indicated a more uniform particle size distribution, reflecting improved reproducibility and controlled drug release, while a higher UI suggested greater variability, potentially affecting the formulation's consistency. The results were expressed as mean ± standard deviation, derived from triplicate batches, providing a comprehensive understanding of the influence of formulation parameters such as stirring speed, emulsifier concentration, and cross-linking conditions on particle size uniformity. This analysis played a vital role in optimizing the microsphere preparation process for desired therapeutic outcomes (Dubey and Parikh, 2004, Shukla et al., 2002).

**Morphology study of microspheres**

The surface morphology and structural characteristics of the prepared microspheres were analyzed using Scanning Electron Microscopy (SEM), specifically employing the JSM-5610 model from Tokyo, Japan. This technique was utilized to examine the shape, surface texture, and overall structural integrity of the microspheres, providing critical insights into the effects of formulation and process parameters on their physical attributes. To prepare the microspheres for SEM analysis, a small quantity of the dried sample was mounted on aluminum stubs using double-sided adhesive carbon tape. The samples were then sputter-coated with a thin layer of gold using a vacuum sputter coater to enhance conductivity and ensure clear imaging during the SEM procedure. Once prepared, the samples were placed into the SEM chamber, and micrographs were captured at various magnifications to observe surface features such as smoothness, porosity, and any evidence of cracks or deformities. The obtained SEM images were analyzed to evaluate the consistency of the microspheres' morphology, which directly impacts drug release behavior, stability, and overall formulation performance. The results provided valuable information on the spherical nature of the microspheres, the effectiveness of the emulsification and cross-linking processes, and the uniformity of the coating layer in the case of coated formulations. These observations were correlated with other formulation variables to optimize the preparation process and achieve the desired microsphere characteristics.

**Determination of drug entrapment, loading capacity (LC)**

The drug entrapment efficiency (DEE) and loading capacity (LC) of the microspheres were determined to assess their ability to encapsulate and retain the drug effectively. A precisely weighed sample of drug-loaded microspheres (approximately 10 mg) was dissolved in 10 ml of phosphate buffer (pH 7.4) to release the entrapped drug. The solution was subjected to continuous stirring or ultrasonication for 30 minutes to ensure complete drug extraction. The resulting mixture was filtered through a 0.45 µm membrane filter to remove undissolved particles, leaving a clear solution for analysis. The filtrate was analyzed spectrophotometrically at the drug's maximum absorption wavelength (λmax at 276 nm) using a UV-Visible spectrophotometer. The amount of drug present in the solution was calculated using a pre-constructed calibration curve of the drug in the same solvent. DEE was calculated as the percentage of the encapsulated drug relative to the total amount of drug initially added, while LC was expressed as the percentage of the drug encapsulated relative to the total weight of the microspheres. The results were expressed as mean ± standard deviation from triplicate measurements. Higher DEE values indicated efficient drug entrapment with minimal loss during the formulation process, while higher LC values demonstrated a favorable proportion of drug within the microspheres (Pachuau and Mazumder, 2009, Jose et al., 2011).. These findings were correlated with formulation parameters, such as polymer concentration, emulsifier levels, and cross-linking conditions, to optimize the microsphere formulation and ensure consistent drug delivery performance.

**Percentage yield**

The percentage yield of the microspheres was calculated to evaluate the efficiency of the formulation process and the conversion of raw materials into the final product. Following the preparation, the microspheres were thoroughly washed to remove residual solvents and impurities. The washed microspheres were then air-dried at

30℃ for 24 hours to achieve a constant weight, ensuring accurate measurement. The dried microspheres were carefully weighed using an analytical balance, and the percentage yield was determined using the formula:
Percentage Yield (%) = (Weight of dried microspheres / Total weight of polymer and drug used) × 100
This calculation provided insights into the effectiveness of the emulsification, cross-linking, and recovery processes. A high percentage yield indicated minimal material loss and efficient formulation, while lower yields pointed to potential inefficiencies or losses during preparation. The results were expressed as mean ± standard deviation from triplicate batches to ensure consistency and reliability. These findings helped identify areas for improvement in the formulation process, optimizing material utilization and overall process efficiency.

**FTIR Spectroscopy and DSC Thermogram Analysis**

Fourier Transform Infrared Spectroscopy (FTIR) was employed to comprehensively characterize the microspheres, focusing on potential drug-polymer interactions and compatibility within the formulation. FTIR spectroscopy was used to identify functional groups and detect any possible chemical interactions between the drug and the polymers used in the formulation. Samples of pure Etodolac, the polymers (Chitosan and Eudragit), and the drug-loaded microspheres were scanned individually. The spectra were recorded using an FTIR spectrometer over the range of 4000–400 $cm^{-1}$. The characteristic peaks corresponding to functional groups in Etodolac, such as carbonyl (C=O), hydroxyl (–OH), and aromatic rings, were compared with those in the physical mixture and the formulated microspheres. Any significant shifts or changes in the peak intensities were analyzed to identify interactions or changes in the chemical structure, confirming the compatibility between the drug and the polymers.

**Swelling ratio studies**

Swelling ratio studies were conducted to assess the water uptake capacity of the microspheres, which is a critical parameter influencing their behavior in biological environments and their suitability for controlled drug release. A known weight of dried microspheres (W0W_0W0) was accurately measured and immersed in phosphate buffer solution (pH 7.4) at 37℃ to simulate physiological conditions. The microspheres were allowed to swell for predetermined time intervals, typically ranging from 1 to 4 hours, under gentle agitation to ensure uniform exposure to the buffer. At each time interval, the swollen microspheres were carefully removed, blotted with filter paper to eliminate excess surface water without damaging their structure, and immediately weighed (W1). The swelling ratio (SR) was calculated using the formula SR = W1 − W0 / W0, where W0 is the initial dry weight and W1 is the weight of the swollen microspheres. This calculation provided a quantitative measure of the hydrophilicity of the microspheres and the porosity of their polymeric network. A higher swelling ratio indicated greater water absorption, which is favourable for enhancing drug release in hydrophilic environments, whereas a lower swelling ratio suggested a more tightly cross-linked polymeric network or a hydrophobic surface, supporting sustained drug release. The results, expressed as mean ± standard deviation from triplicate measurements, were analyzed to correlate the swelling behaviour with formulation parameters such as polymer concentration, cross-linking density, and the coating material. These studies offered valuable insights into the optimization of microsphere design to achieve the desired drug release profile, ensuring their effectiveness in drug delivery applications.

**Drug Release Study: Core Microparticle**

The in vitro drug release study of the core microparticles was conducted under conditions simulating different segments of the gastrointestinal (GI) tract to evaluate their release behavior and targeted delivery potential. A known quantity of drug-loaded core microparticles, equivalent to a specific drug dose, was placed in 900 ml of dissolution medium in a USP Type II (paddle) dissolution apparatus maintained at 37 ± 0.5℃ with a stirring speed of 50 rpm. The study began with the microparticles exposed to simulated gastric fluid (pH 1.2) prepared as 0.1N HCl to mimic gastric conditions. The microparticles remained in this medium for 2 hours, during which minimal drug release was expected due to the pH-sensitive nature of the formulation. Subsequently, the pH of the dissolution medium was adjusted to 4.5 using an appropriate buffer to simulate duodenal conditions, and the release study continued for another 2 hours. Finally, the pH was adjusted to 7.4 to replicate the environment of the distal ileum and colon. The release study proceeded for the remaining duration, typically up to 12 or 24 hours, to evaluate the drug release in these regions. At predefined time intervals, 5 ml samples of the dissolution medium were withdrawn, filtered through a 0.45 µm membrane filter, and replaced with an equal volume of fresh pre-warmed medium to maintain sink conditions. The drug content in the samples was quantified spectrophotometrically at the λmax of Etodolac (approximately 276 nm), and the cumulative percentage of drug released was calculated using a calibration curve.

The release profile demonstrated minimal drug release in acidic conditions (pH 1.2 and pH 4.5), simulating the stomach and duodenum, respectively, while significant release was observed at pH 7.4, corresponding to the distal ileum and colon. This confirmed the pH-sensitive behavior of the core microparticles, designed for targeted and controlled drug delivery in the lower GI tract. The release data were further analyzed using kinetic models such as zero-order, first-order, Higuchi, and Korsmeyer-Peppas equations to determine the mechanism of drug release, with the best-fit model identified based on regression coefficient (R2) values. These findings

validated the suitability of the core microparticles for chronotherapeutic applications, ensuring precise drug release at the desired site and time (Jose et al., 2011).

**Drug Release Study: Coated Microparticle**

The in vitro drug release study of the coated microparticles was performed to evaluate the impact of the pH-sensitive Eudragit coating on the drug release profile and its suitability for targeted delivery. The study simulated the sequential conditions of the gastrointestinal (GI) tract, assessing the ability of the coated microparticles to delay release in the stomach and initiate controlled release in the distal GI regions. The study commenced by exposing a known quantity of coated drug-loaded microparticles to simulated gastric fluid (pH 1.2), prepared as 0.1N HCl, for 2 hours to mimic stomach conditions. Minimal drug release was expected in this phase due to the protective nature of the Eudragit coating, which remains insoluble in acidic environments. After 2 hours, the pH of the medium was adjusted to 4.5 using an appropriate buffer to simulate simulated duodenum fluid (pH 4.5), and the release study was continued for another 2 hours. During this phase, the coating was expected to remain intact, preventing significant drug release.

Finally, the medium's pH was adjusted to 7.4 to simulate conditions in the distal ileum and colon (pH 7.4), where the Eudragit coating dissolves, facilitating drug release. The study continued for up to 12 or 24 hours, depending on the experimental design. At predetermined intervals, 5 ml samples of the dissolution medium were withdrawn, filtered through a 0.45 µm membrane filter, and replaced with an equal volume of fresh medium to maintain sink conditions. The drug content in the samples was measured spectrophotometrically at the λmax of Etodolac (approximately 273–276 nm), and the cumulative percentage of drug released was calculated. The release profile revealed negligible drug release at pH 1.2 and pH 4.5, confirming the coating's ability to protect the drug from premature release in the stomach and duodenum. A significant and sustained release was observed at pH 7.4, demonstrating the efficacy of the Eudragit coating in ensuring targeted drug delivery to the distal GI tract. The data were analyzed using various kinetic models, such as zero-order, first-order, Higuchi, and Korsmeyer-Peppas, to understand the release mechanism, with the best-fit model determined based on regression coefficient (R2R^2R2) values. These findings validated the coated microparticles' potential for pH-sensitive and chronotherapeutic drug delivery, optimizing therapeutic outcomes by ensuring precise release at the desired site and time.

**Kinetics of drug release from Microparticle**

The drug release kinetics of the microparticles were analyzed to understand the mechanism governing the release profile and to evaluate the efficiency of the formulation in achieving controlled or targeted drug delivery. The cumulative drug release data obtained from the in vitro release studies were fitted into various mathematical models to identify the best-fit kinetic model and the drug release mechanism.

***Mathematical Models:***

1. ***Zero-Order Kinetics****:*

$Qt=Q0+k0t$

This model describes a system where the drug release rate is constant over time, irrespective of the drug concentration, indicating a controlled release mechanism.

2. **First-Order Kinetics**:

$Ln\ Qt = ln\ Q0 + k1t$

This model assumes the drug release rate is proportional to the remaining drug concentration, typical of diffusion-controlled systems.

3. **Higuchi Model**:

$Qt=kH\ \sqrt{t}$

This model describes drug release as a diffusion process based on Fick's law, where the release is proportional to the square root of time.

4. **Korsmeyer-Peppas Model**:

$Qt / Q\infty = k_k t^n$

This semi-empirical model is used to identify the mechanism of drug release. The release exponent (nnn) indicates the mechanism:

- $n<0.5$: Fickian diffusion.
- $0.5\leq n<1.0$: Non-Fickian (anomalous) transport.
- $n=1.0$: Zero-order release.
- $n>1.0$: Super Case-II transport.

5. **Hixson-Crowell Model**:

$Q_0^{1/3} – Q_t^{1/3} =k_H t$

This model applies to systems where drug release occurs due to a change in surface area and diameter of the particles.

***Procedure:***

The cumulative drug release data were plotted against time for each of these models using specialized software or spreadsheets. The regression coefficient (R2) was calculated for each model, and the model with the highest R2 value was considered the best fit. For the Korsmeyer-Peppas model, the value of the release exponent (n) was analyzed to interpret the release mechanism. The analysis of the drug release kinetics provided critical insights into the underlying mechanisms of drug release from the microparticles. A fit to the Higuchi model suggested diffusion-controlled release, while a Korsmeyer-Peppas fit with nnn values between 0.5 and 1.0 indicated a combination of diffusion and polymer relaxation. The results helped validate the formulation design, ensuring the microparticles achieved the desired release characteristics for effective therapeutic outcomes. These findings also guided further optimization of the formulation parameters to refine the drug delivery system.

**Statistical Analysis**

Statistical analysis was conducted to ensure the reliability and significance of the experimental data. Results from studies such as drug release, particle size, and entrapment efficiency were expressed as mean ± standard deviation (n=3). One-way ANOVA was employed to evaluate the impact of formulation variables, with a ppp-value < 0.05 considered significant. Post hoc tests like Tukey's or Bonferroni correction were used to identify specific differences between groups. Regression analysis was applied to kinetic modeling to determine the best-fit release mechanism based on the highest R2 value. Student's t-test was used for comparing two datasets, such as coated versus uncoated microparticles. Graphical representations, including bar charts and line graphs with error bars, were created to visualize trends. Software tools such as SPSS and GraphPad Prism facilitated detailed statistical evaluations. These analyses confirmed the reproducibility of the results, highlighted significant differences across formulations, and validated the optimization process, ensuring the development of an effective and reliable drug delivery system.

## 3. RESULTS AND DISCUSSION

**Determination of mean particle size and particle size distribution**

The mean particle size and distribution of the different formulations reflect the influence of drug-to-polymer ratios, stirring speed, and coating type on particle characteristics. For uncoated formulations (CTF-1 to CTF-8), an increase in stirring speed significantly reduces particle size. For example, CTF-1 (600 rpm) exhibited a mean size of 47.70 ± 1.74 µm, while CTF-4 (2400 rpm) achieved the smallest size of 20.52 ± 0.79 µm, highlighting the role of shear forces in minimizing particle aggregation. Formulations with higher drug-to-polymer ratios, such as CTF-5 to CTF-8, display a moderate increase in particle size, likely due to the formation of a thicker polymeric matrix, with CTF-8 (1:5) reaching 30.43 ± 1.33 µm. Coated formulations (ECCTF-1 to ECCTF-3) exhibit significantly larger particle sizes compared to their uncoated counterparts due to the addition of Eudragit as a coating material. ECCTF-1, with a core-to-coat ratio of 1:8, demonstrated the largest particle size (105.45 ± 6.74 µm), reflecting a thicker and more uniform coating layer, while ECCTF-3 (1:5, Eudragit L 100) exhibited a slightly smaller size of 93.59 ± 4.52 µm, attributable to differences in polymer composition and coat thickness. These findings emphasize the critical role of process parameters and formulation composition in controlling particle size and distribution, which directly impact drug release, stability, and bioavailability. Smaller particle sizes are advantageous for rapid dissolution and release, while larger, coated particles are more suited for controlled or delayed-release systems, tailored to specific therapeutic needs (Lorenzo-Lamosa et al., 1998).

**Table 2.** Mean particle size and particle size distribution of different formulations.

| Formulation | Drug: Polymer | Stirring Speed (rpm) | Mean Particle Size (µm) |
|---|---|---|---|
| CTF-1 | 1:1 | 600 | 47.70 ± 1.74 |
| CTF-2 | 1:1 | 1200 | 32.20 ± 1.01 |
| CTF-3 | 1:1 | 1800 | 21.82 ± 0.84 |
| CTF-4 | 1:1 | 2400 | 20.52 ± 0.79 |
| CTF-5 | 1:2 | 1500 | 24.21 ± 0.98 |
| CTF-6 | 1:3 | 1500 | 29.83 ± 0.99 |
| CTF-7 | 1:4 | 1500 | 29.88 ± 0.99 |
| CTF-8 | 1:5 | 1500 | 30.43 ± 1.33 |
| **Coated** | **Core: Coat** | | |
| ECCTF-1 (Eudragit S 100) | 1:8 | 1500 | 105.45 ± 6.74 |
| ECCTF-2 (Eudragit S 100) | 1:6 | 1500 | 93.48 ± 5.12 |
| ECCTF-3 (Eudragit L 100) | 1:5 | 1500 | 93.59 ± 4.52 |

**Uniformity index**

The uniformity index (UI) data highlight the influence of drug-to-polymer ratios, stirring speed, and coating materials on the consistency of particle size distribution across formulations. For uncoated formulations (CTF-1 to CTF-8), a decrease in UI is observed with higher drug-to-polymer ratios. Formulations such as CTF-6, CTF-7, and CTF-8 exhibit the lowest UI values (0.999 ± 0.05, 0.986 ± 0.03, and 0.977 ± 0.13, respectively), reflecting a more uniform particle size distribution. These findings indicate that higher polymer concentrations create a denser matrix, reducing variability in particle size. Stirring speed also influences uniformity, with moderate speeds (e.g., 1500 rpm) producing lower UI values compared to extremes. For instance, CTF-4, processed at 2400 rpm, shows a significantly higher UI (2.977 ± 0.10), suggesting that excessive shear forces may lead to inconsistent particle formation. Coated formulations (ECMSF-1 to ECMSF-3) exhibit moderate UI values (1.109 ± 0.08 to 1.242 ± 0.09), attributed to the additional coating material. ECMSF-1 (Eudragit S 100, 1:8) shows the most uniform distribution among coated formulations, indicating that higher coat-to-core ratios enhance particle consistency. However, differences between Eudragit S 100 and L 100 appear minimal in terms of uniformity. Overall, the results suggest that optimized drug-to-polymer ratios, moderate stirring speeds, and precise coating processes are essential for achieving uniform particle size distribution. Uniformity plays a critical role in ensuring predictable drug release, reproducibility, and improved therapeutic outcomes (Dubey and Parikh, 2004, Jeyanthi et al., 1997).

**Table 3.** Uniformity index of different formulations.

| Formulation | Drug: Polymer | Stirring Speed (rpm) | Uniformity Index (UI) |
|---|---|---|---|
| CTF-1 | 1:1 | 600 | 2.270 ± 0.10 |
| CTF-2 | 1:1 | 1200 | 2.218 ± 0.10 |
| CTF-3 | 1:1 | 1800 | 2.175 ± 0.11 |
| CTF-4 | 1:1 | 2400 | 2.977 ± 0.10 |
| CTF-5 | 1:2 | 1500 | 1.285 ± 0.07 |
| CTF-6 | 1:3 | 1500 | 0.999 ± 0.05 |
| CTF-7 | 1:4 | 1500 | 0.986 ± 0.03 |
| CTF-8 | 1:5 | 1500 | 0.977 ± 0.13 |
| **Coated** | **Core: Coat** | | |
| ECMSF-1 (Eudragit S 100) | 1:8 | 1500 | 1.109 ± 0.08 |
| ECMSF-2 (Eudragit S 100) | 1:6 | 1500 | 1.242 ±0.09 |
| ECMSF-3 (Eudragit L 100) | 1:5 | 1500 | 1.211 ± 0.07 |

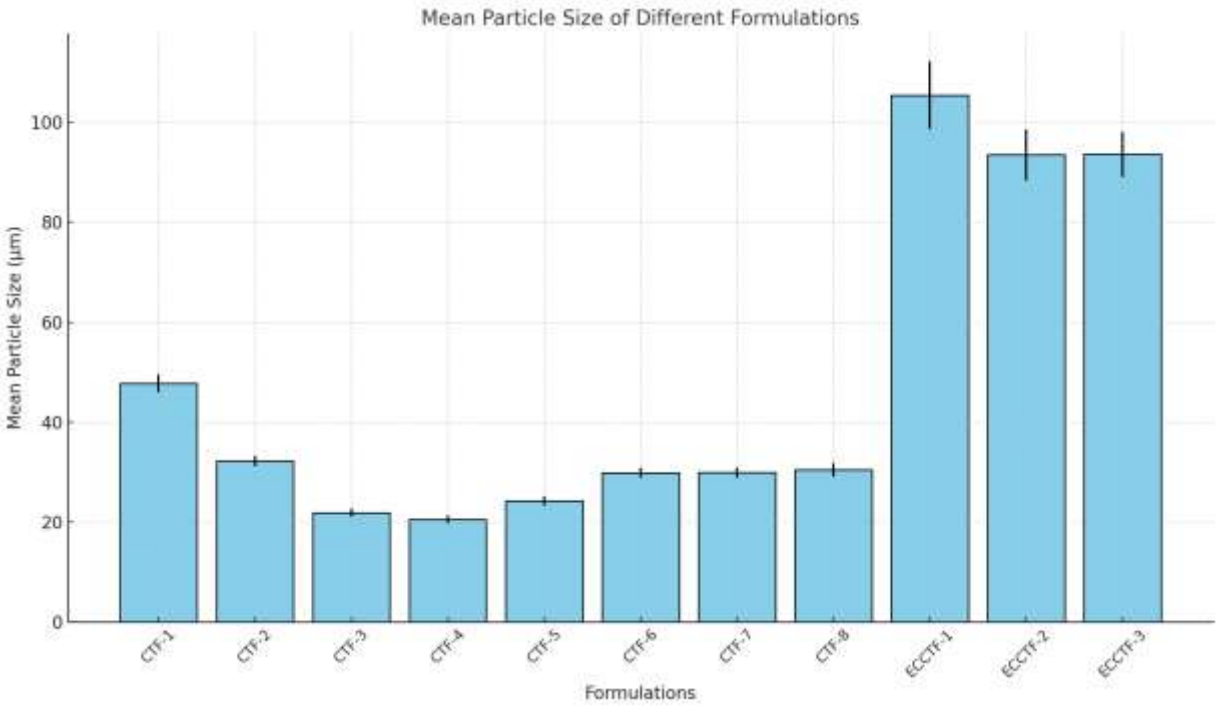


**Figure 1.** Frequency Destribution of of different formulation.

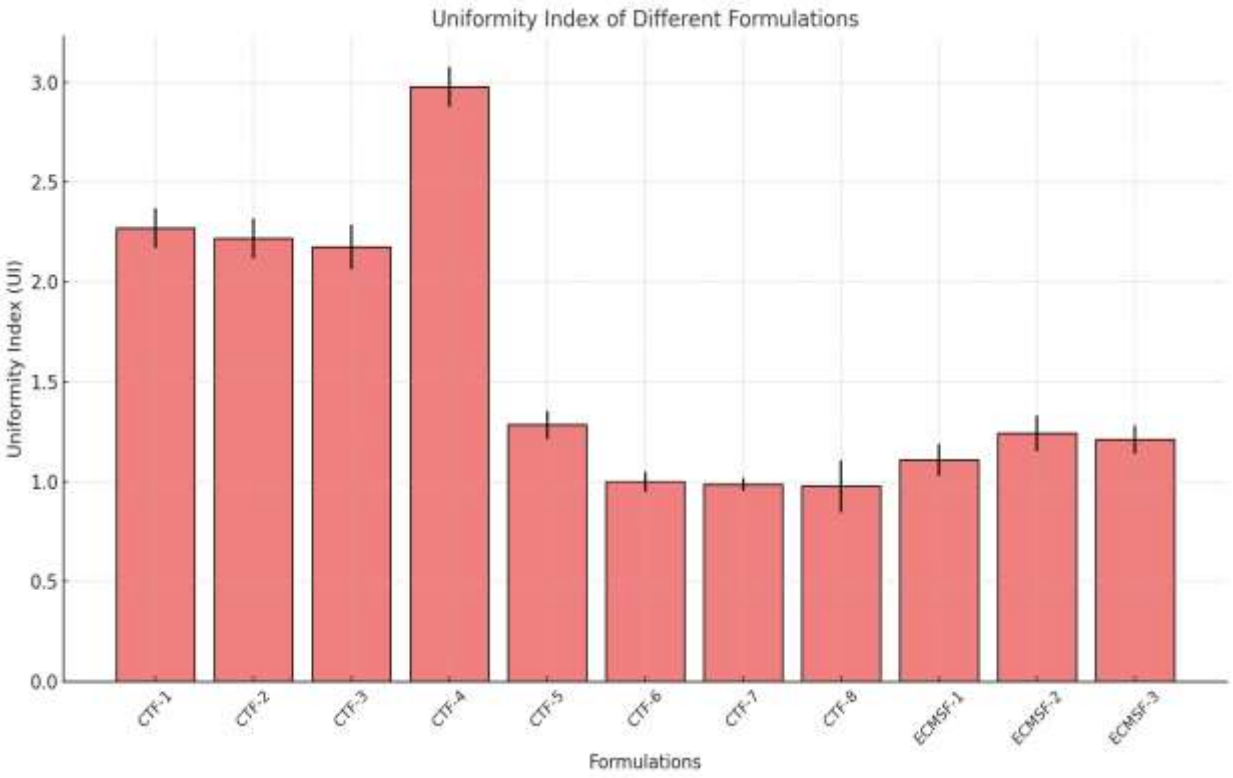


**Figure 2.** Uniformity Index (UI) of of different formulation

**Morphology study of microspheres**

The scanning electron photomicrographs depicted in Figure 3 illustrate the distinct morphological differences between the core and coated microparticles. The core microparticles (left) exhibit a relatively smooth surface with minor irregularities, indicative of a well-formed polymeric matrix. In contrast, the coated microparticles (right) demonstrate a uniform and thicker outer layer, confirming the successful application of the Eudragit coating. The coating appears continuous and devoid of visible cracks, highlighting its integrity and potential to provide controlled or delayed drug release. These structural characteristics align with the intended design parameters, ensuring the functional performance of the microparticles in drug delivery applications.

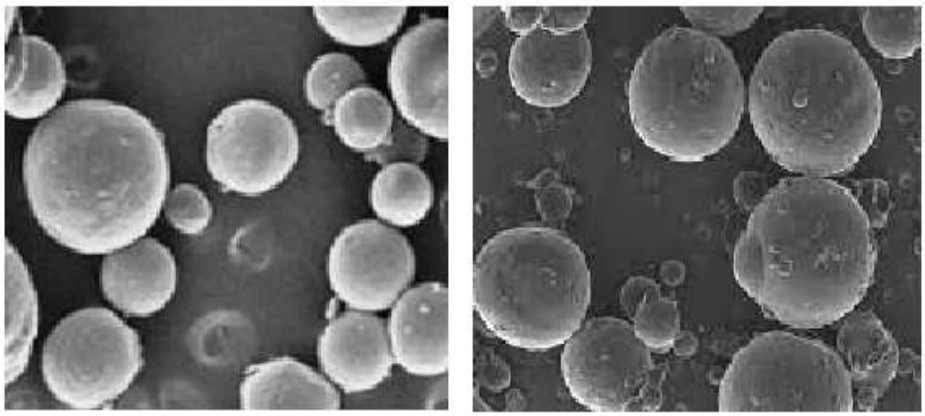

**Figure 3.** Scanning electron photomicrograph of core microparticle (Left) and coated microparticle (Right).

**Percentage yield**

The percentage yield data across formulations reflect the influence of rotation speed, drug-to-polymer ratio, and coating on the efficiency of microparticle production. Uncoated formulations (CTF-1 to CTF-4) display moderate yields, ranging from 75.90 ± 0.83% to 78.98 ± 0.99%. Notably, CTF-3 at 1800 rpm achieved the highest yield in this group, suggesting that moderate-to-high rotation speeds optimize the emulsification process

while minimizing material loss. However, the yield slightly decreased for CTF-4 at 2400 rpm, indicating that excessive speed may lead to instability in the emulsion or loss during processing. Formulations with higher drug-to-polymer ratios (CTF-5 to CTF-8) and coated formulations (ECCTF-1 to ECCTF-3) demonstrated significantly higher yields, with CTF-7 and ECCTF-2 achieving maximum yields of 94.05 ± 0.70% and 94.87 ± 0.32%, respectively. These findings suggest that higher polymer concentrations and coating enhance yield by providing structural stability and reducing material loss during processing. Overall, the results highlight that optimizing rotation speed and polymer concentration is critical for maximizing yield while maintaining formulation integrity. Coated formulations achieved comparable or higher yields, demonstrating the feasibility of coating processes without significant losses.

**Table 4.** Percentage yield of different formulation.

| Formulation | Rotation Speed (R.P.M) | % yield |
|---|---|---|
| CTF-1 | 600 | 76.20 ± 0.52 |
| CTF-2 | 1200 | 77.90 ± 0.43 |
| CTF-3 | 1800 | 78.98 ± 0.99 |
| CTF-4 | 2400 | 75.90 ± 0.83 |
| CTF-5 | 1500 | 82.99 ± 0.45 |
| CTF-6 | 1500 | 88.46 ± 0.42 |
| CTF-7 | 1500 | 94.05 ± 0.70 |
| CTF-8 | 1500 | 92.61 ± 0.70 |
| ECCTF-1 | 1500 | 92.83 ± 0.93 |
| ECCTF-2 | 1500 | 94.87 ± 0.32 |
| ECCTF-3 | 1500 | 93.89 ± 0.49 |

**Loading capacity and Encapsulation efficiency**

The loading capacity and encapsulation efficiency data reveal the impact of rotation speed, polymer concentration, and coating on the performance of the microparticle formulations. For uncoated formulations (CTF-1 to CTF-4), both loading capacity and encapsulation efficiency increased with higher rotation speeds. CTF-4, prepared at 2400 rpm, achieved the highest loading capacity (31.54 ± 0.47%) and encapsulation efficiency (82.56 ± 0.72%) among this group, indicating that high shear forces enhance the uniform distribution of the drug within the polymer matrix. Formulations with higher polymer concentrations (CTF-5 to CTF-8) showed a decline in loading capacity (e.g., 11.20 ± 0.25% for CTF-8) but a significant improvement in encapsulation efficiency, reaching a maximum of 92.26 ± 0.61% for CTF-8. This suggests that higher polymer content reduces drug loading but enhances encapsulation due to the denser polymer matrix providing a more protective environment for the drug. Coated formulations (ECCTF-1 to ECCTF-3) exhibited moderate loading capacities (13.04 ± 0.21% to 13.56 ± 0.11%) but the highest encapsulation efficiencies, with ECCTF-3 achieving a maximum of 98.34 ± 0.09%. The coating process likely prevents drug leakage and improves encapsulation by adding an additional barrier layer. In conclusion, optimizing rotation speed and polymer concentration is crucial for balancing loading capacity and encapsulation efficiency. While uncoated formulations are effective for high drug loading, coated formulations excel in maximizing encapsulation, making them ideal for applications requiring controlled and sustained drug release.

**Table 5.** Loading Capacity and Encapsulation efficiency of different formulation.

| Formulation | Rotation Speed (R.P.M) | Loading capacity (%) | Encapsulation efficiency (%) |
|---|---|---|---|
| CTF-1 | 600 | 27.54 ± 0.30 | 75.54 ± 0.81 |
| CTF-2 | 1200 | 28.54 ± 0.39 | 77.84 ± 0.70 |
| CTF-3 | 1800 | 29.86 ± 0.36 | 81.92 ± 0.89 |
| CTF-4 | 2400 | 31.54 ± 0.47 | 82.56 ± 0.72 |
| CTF-5 | 1500 | 21.30 ± 0.34 | 83.24 ± 1.03 |
| CTF-6 | 1500 | 16.08 ± 0.11 | 83.24 ± 0.74 |
| CTF-7 | 1500 | 13.10 ± 0.89 | 89.54 ± 0.80 |
| CTF-8 | 1500 | 11.20 ± 0.25 | 92.26 ± 0.61 |
| ECCTF-1 | 1500 | 13.04 ± 0.21 | 95.58 ± 0.51 |
| ECCTF-2 | 1500 | 13.56 ± 0.11 | 98.00 ± 0.61 |
| ECCTF-3 | 1500 | 13.52 ± 0.23 | 98.34 ± 0.09 |

**FTIR Study**

The FTIR spectra of chitosan, Etodolac sulfate, and the formulated microparticles were analyzed to assess potential interactions between the components. The spectrum of chitosan (a) exhibited characteristic peaks, including a broad absorption band around 3420 $cm^{-1}$ for –OH and –NH stretching, and peaks at 1650 $cm^{-1}$ and 1380 $cm^{-1}$ corresponding to –C=O stretching of amide I and $–CH_3$ bending, respectively. Etodolac sulfate (b) showed distinct peaks for its functional groups, including –C=O stretching near 1720 $cm^{-1}$ and –NH bending around 1570 $cm^{-1}$. In the spectrum of the microparticles (c), all major peaks from chitosan and Etodolac sulfate were retained, though slight shifts or changes in peak intensity were observed. These changes suggest physical interactions, such as hydrogen bonding, between the drug and polymer during formulation. Importantly, no new peaks indicative of chemical incompatibility or degradation products were detected, confirming that the drug remained stable and compatible with the excipients in the microparticle system. This ensures the structural integrity and functionality of the final formulation.

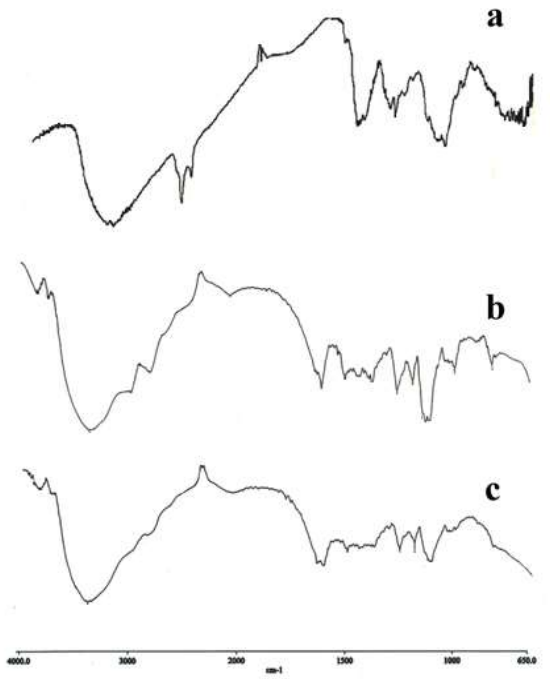


**Figure 4.** FTIR Spectra of Chitosan (a), Etodolac sulphate (b) and microparticle (c).

**Swelling study**

The swelling behavior of the formulations (CTF-1 to CTF-8) over time demonstrates clear differences influenced by polymer concentration and cross-linking density. During the initial phase (0–1 hour), all formulations showed rapid swelling, attributed to the hydrophilic nature of chitosan and the availability of free spaces in the polymer matrix. Formulations CTF-7 and CTF-8 exhibited the highest swelling percentages (510% and 560%, respectively), reflecting their higher polymer concentrations and lower cross-linking densities, which allow greater water uptake. In the progressive swelling phase (1–5 hours), the swelling rate slowed as the polymer matrices absorbed more water. Formulations CTF-5 to CTF-8 maintained higher swelling capacities, while CTF-1 to CTF-4 exhibited lower percentages, suggesting tighter polymer networks. Beyond 6 hours, all formulations reached equilibrium, with CTF-7 and CTF-8 stabilizing at 560% and 590%, respectively, while CTF-1 leveled off at 390%. This behavior highlights the role of polymer concentration in dictating swelling capacity, with higher concentrations enabling larger water uptake. These findings suggest that formulations with lower swelling percentages, such as CTF-1 to CTF-4, may be suitable for sustained drug release, whereas higher swelling formulations, such as CTF-5 to CTF-8, are more appropriate for rapid or burst drug release applications. The results underscore the importance of optimizing polymer and cross-linker concentrations to achieve desired drug delivery outcomes (Roy et al., 2009, Shivakumar et al., 2010).

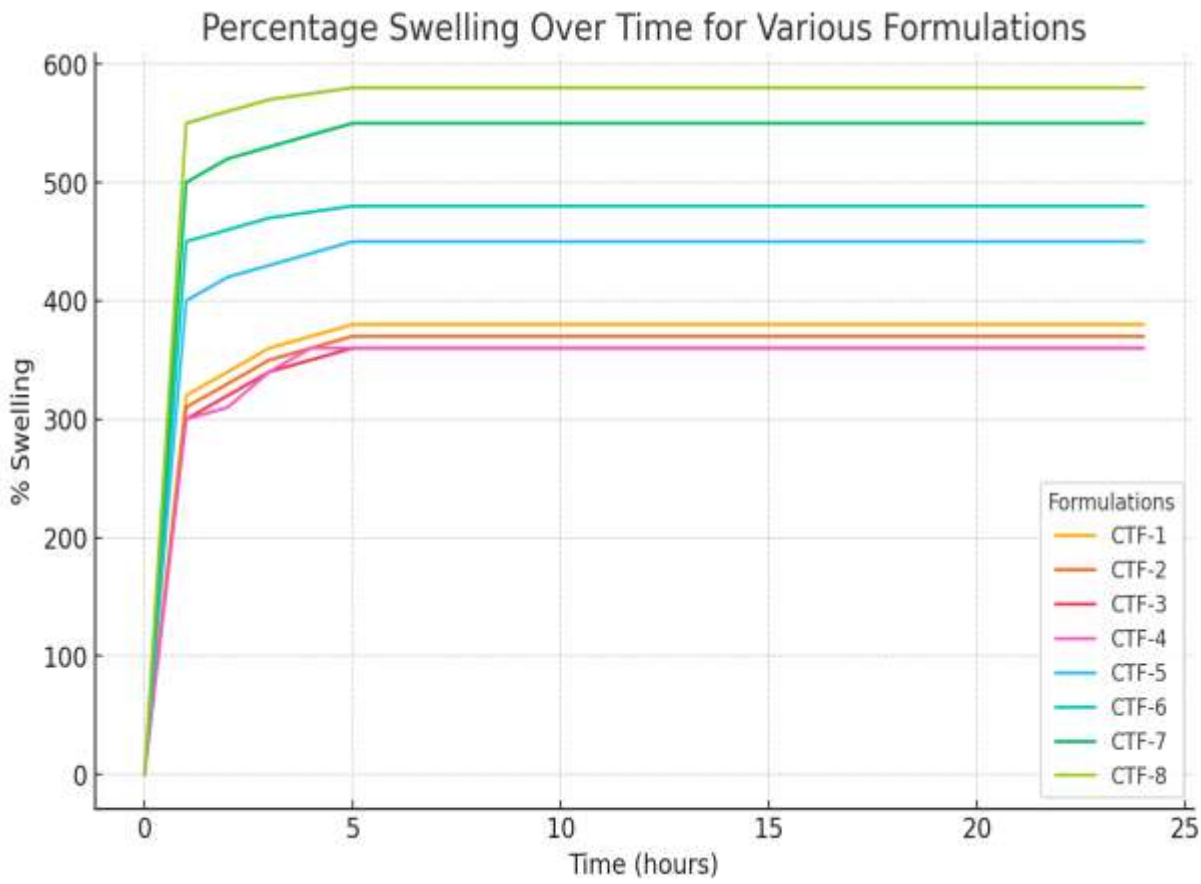


**Figure 5.** Swelling profile of core microparticle at pH 7

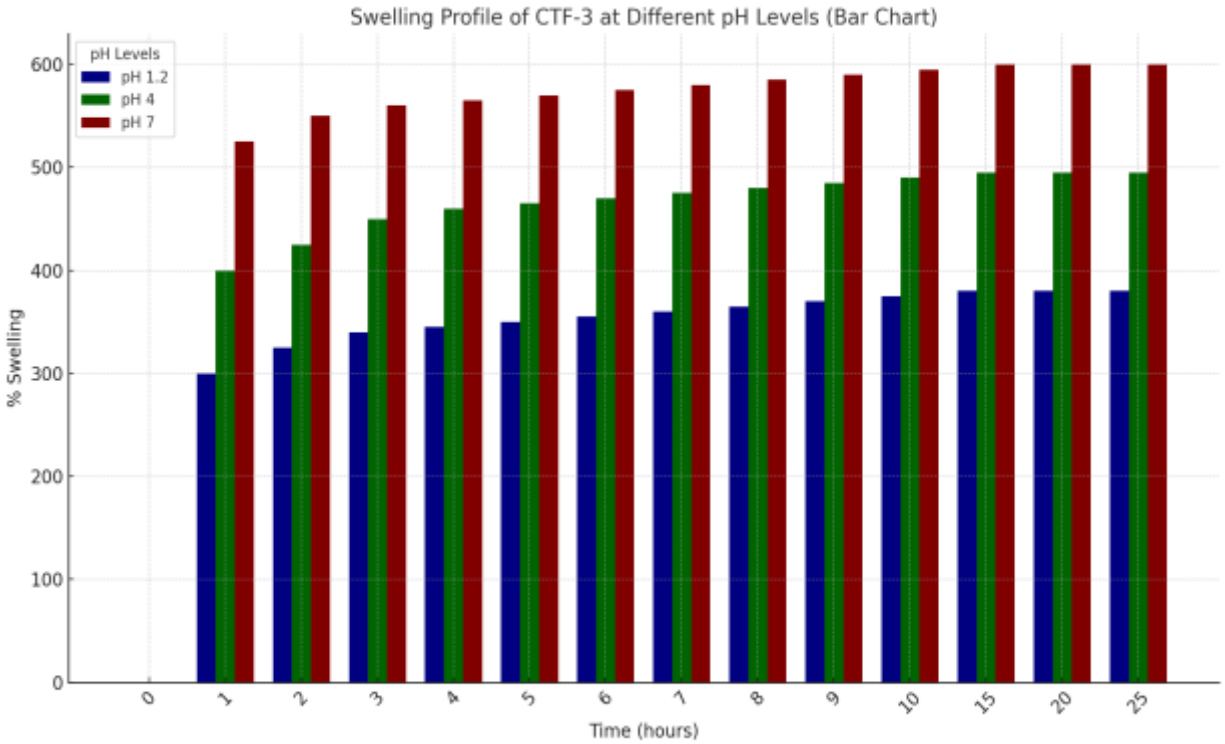


**Figure 6.** Swelling profile of CTF-3 at different pH (pH 1.2, pH 4 and pH 7).

**Drug release from core microparticle**

The cumulative drug release profiles for the formulations (CTF-1 to CTF-8) demonstrate distinct release behaviors influenced by their composition and design parameters. Initially, all formulations exhibited a gradual release, with CTF-4 showing the highest early release due to its relatively faster dissolution properties. Formulations with lower drug release rates, such as CTF-7 and CTF-8, displayed a more sustained release pattern, which may be attributed to higher polymer content or stronger cross-linking, limiting drug diffusion. By 10 hours, most formulations achieved significant drug release, with CTF-4 and CTF-3 reaching 105% and 102% cumulative release, respectively, reflecting faster release kinetics suitable for immediate therapeutic needs. In contrast, formulations like CTF-8 exhibited a prolonged release profile, achieving only 87% at the same time point, indicating their suitability for extended-release applications. The stacked area plot highlights the progressive contribution of each formulation over time, emphasizing their varied release patterns. These results underscore the importance of tailoring formulation parameters to meet specific therapeutic goals, such as immediate or sustained drug delivery.

**Drug release from coated microsphere**

The drug release profiles from the coated microspheres (ECCTF-1, ECCTF-2, and ECCTF-3) reveal distinct behaviors influenced by the coating composition and thickness. Initially, all formulations exhibit minimal drug release, particularly in the first six hours, demonstrating the efficacy of the coating in preventing premature drug diffusion. ECCTF-3 shows the earliest release, with 17% at 2 hours and a gradual increase to 44% by 6 hours, suggesting a thinner or more permeable coating compared to ECCTF-1 and ECCTF-2. By 7 hours, ECCTF-1 and ECCTF-2 begin releasing the drug, with ECCTF-1 reaching 24% and ECCTF-2 at 14%, indicating their more robust coating properties. As time progresses, ECCTF-3 achieves the highest cumulative release, reaching 104% by 10 hours, suitable for formulations requiring rapid release after a lag phase. In contrast, ECCTF-1 and ECCTF-2 demonstrate more controlled release, with ECCTF-1 achieving 75% by 11 hours, indicating its potential for sustained delivery. These differences emphasize the importance of coating parameters in tailoring drug release to meet specific therapeutic needs, such as delayed or controlled delivery.

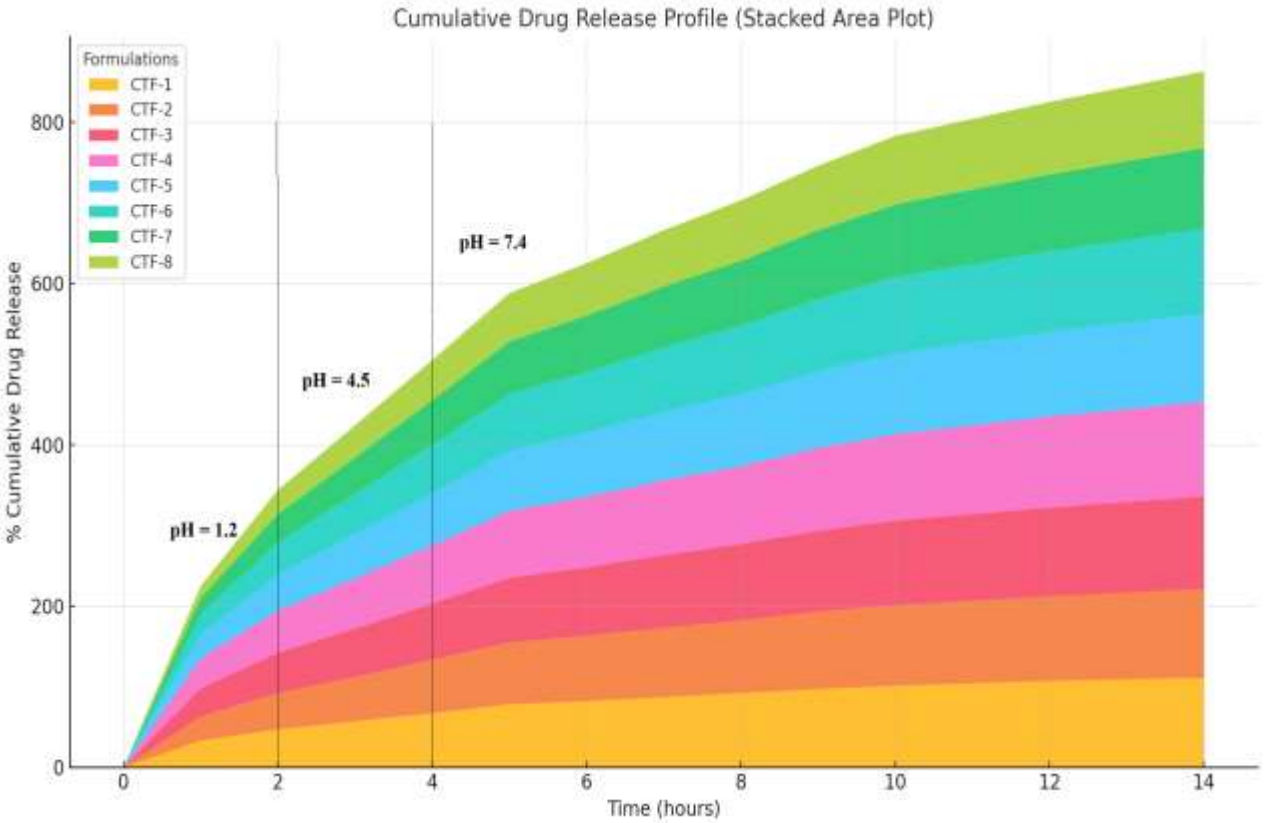


**Figure 7.** Drug release of different core microparticle at pH 1.2(2 hr),pH 4.5 (2 hr) and pH 7.4.

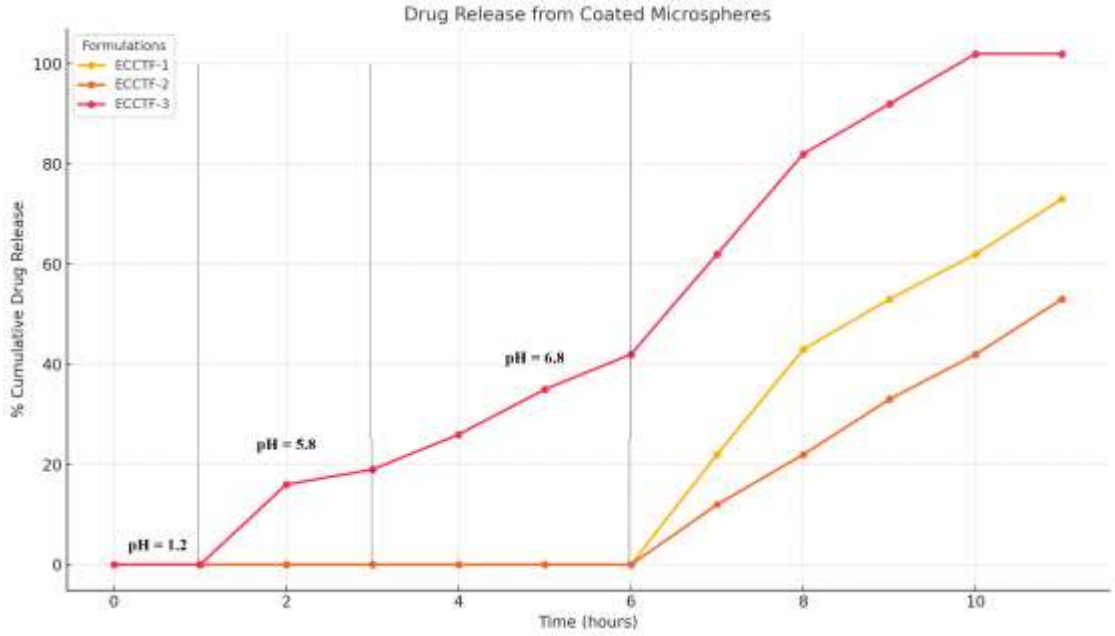


**Figure 8.** Drug release of different Coated microparticle at pH 1.2 (2 hr), pH 5.8 (2 hr), pH 6.8 (2 hr) and pH 7.4.

**Drug release Kinetics**

The kinetic modelling of drug release from the formulations (CTF-1 to CTF-8 and ECCTF-1 to ECCTF-3) highlights distinct behaviours based on their composition and design, with insights drawn from the regression coefficients (r2) and kinetic constants across various models.

1. **Zero-Order Kinetics**: Most formulations exhibit moderate r2 values for zero-order kinetics (0.8358–0.9553), with ECCTF-3 showing the highest (r2=0.9553). This indicates a controlled and sustained release pattern, particularly for formulations like ECCTF-3, which release drugs at a consistent rate, independent of drug concentration.
2. **First-Order Kinetics**: First-order kinetics generally show lower r2 values for CTF formulations compared to zero-order. However, ECCTF formulations, especially ECCTF-3 (r2=0.9591), fit well within this model, suggesting release dependent on the remaining drug concentration, making them suitable for prolonged release in coated systems.
3. **Higuchi Model**: The Higuchi model consistently shows the highest r2 values for all formulations (0.9875–0.9954), indicating a predominantly diffusion-controlled release mechanism. This is particularly evident in uncoated formulations (CTF-1 to CTF-8), where the release rate is proportional to the square root of time, highlighting the impact of the polymeric matrix in regulating drug diffusion.
4. **Korsmeyer-Peppas Model**: The Korsmeyer-Peppas model provides the best fit (r2 values up to 0.9977) for most formulations, particularly CTF-3 and CTF-4. The release exponent (nnn) values for these formulations are below 0.5, suggesting Fickian diffusion as the predominant mechanism. In contrast, ECCTF-2 exhibits a higher n value (2.2059), indicating non-Fickian or anomalous transport, combining both diffusion and polymer relaxation effects, likely due to the coating's delayed release behaviour.
5. **Comparison Between Coated and Uncoated Formulations**: Uncoated formulations (CTF-1 to CTF-8) predominantly follow Higuchi diffusion due to the hydrophilic nature of the matrix, with higher n values in formulations like CTF-7 and CTF-8 (n>0.5) indicating a transition to non-Fickian transport. Coated formulations (ECCTF-1 to ECCTF-3), particularly ECCTF-3, exhibit a significant shift towards controlled release (high zero-order r2=0.9553) and prolonged drug release, supported by their Peppas exponent values.

The study highlights that uncoated formulations predominantly follow Higuchi and Fickian diffusion mechanisms, suitable for immediate to sustained release. In contrast, coated formulations provide more controlled and prolonged release, suitable for applications requiring delayed release. The choice of formulation can be tailored based on therapeutic needs, leveraging insights from kinetic modelling to achieve desired drug release profiles.

**Table 6.** Drug Release and kinetic of different formulation.

| | Zero order | | First Order | | Higuchi | | Pappas | |
|---|---|---|---|---|---|---|---|---|
| **Formulation** | **r2** | **K0** | **r2** | **Kf** | **r2** | **Kh** | **r2** | **n** |

| | | | | | | | | |
|---|---|---|---|---|---|---|---|---|
| CTF-1 | 0.8358 | 7.0654 | 0.4922 | 34.3232 | 0.9926 | 33.3012 | 0.9963 | 0.4659 |
| CTF-2 | 0.8862 | 7.0842 | 0.4744 | 31.6171 | 0.9919 | 32.7937 | 0.9941 | 0.4803 |
| CTF-3 | 0.8785 | 7.2313 | 0.5029 | 36.7361 | 0.9927 | 34.4459 | 0.9977 | 0.4571 |
| CTF-4 | 0.8716 | 7.3180 | 0.5134 | 38.6979 | 0.9907 | 35.2844 | 0.9974 | 0.4475 |
| CTF-5 | 0.8942 | 7.0912 | 0.4719 | 31.5992 | 0.9950 | 32.6150 | 0.9964 | 0.4855 |
| CTF-6 | 0.9090 | 6.9498 | 0.4393 | 26.3964 | 0.9954 | 30.7833 | 0.9947 | 0.5175 |
| CTF-7 | 0.9227 | 6.8088 | 1.0188 | 0.1996 | 0.9934 | 28.9512 | 0.9924 | 0.5540 |
| CTF-8 | 0.9327 | 6.6995 | 1.0199 | 0.1785 | 0.9875 | 27.2565 | 0.9879 | 0.5952 |
| ECCTF-1 | 0.8823 | 7.0689 | 0.8802 | 0.00002 | 0.6646 | 14.4376 | 0.9132 | 1.9422 |
| ECCTF-2 | 0.8752 | 5.0074 | 0.8731 | 0.000008 | 0.6393 | 10.0307 | 0.9439 | 2.2059 |
| ECCTF-3 | 0.9553 | 9.0371 | 0.9591 | 0.0173 | 0.8670 | 25.7939 | 0.9343 | 1.0385 |

## 4. CONCLUSIONS

The development of Etodolac-loaded microparticles for chronomodulated delivery demonstrated significant potential for optimized rheumatoid arthritis management. The coated microparticles exhibited superior encapsulation efficiencies (up to 98.34 ± 0.09%) and sustained release profiles, making them suitable for aligning drug release with the circadian rhythm of rheumatoid arthritis symptoms. Morphological analysis confirmed uniformity and structural integrity, while FTIR analysis validated chemical stability and compatibility between the drug and excipients. Uncoated microparticles provided faster release, whereas coated formulations demonstrated prolonged drug release, following zero-order and Higuchi kinetics. ECCTF-3 emerged as the most promising formulation due to its excellent encapsulation efficiency and extended release characteristics. The study underscores the importance of optimizing polymer ratios, stirring speeds, and coating parameters to achieve precise chronomodulated drug delivery. This work establishes a foundation for further exploration of Etodolac-loaded systems in chronotherapeutic applications, offering a promising strategy for improving symptom control and patient adherence in rheumatoid arthritis.

## REFERENCES


[1] AODAH, A. H. Y. 2009. *Design and evaluation of Chronotherapeutic drug delivery Systems for the treatment of Nocturnal asthma.* Master Degree, King Saud University.

[2] BALFOUR, J. A. & BUCKLEY, M. M. 1991. Etodolac. A reappraisal of its pharmacology and therapeutic use in rheumatic diseases and pain states. *Drugs,* 42**,** 274-99.

[3] BOGIN, R. M. & BALLARD, R. D. 1992. Treatment of nocturnal asthma with pulsed release albuterol. *Chest,* 102**,** 362-366.

[4] COCHRANE, G. M. & CLARK, T. J. H. 1975. A survey of asthma mortality in patients between 35 and 65 years in the greater London hospitals in 1971. *Thorax,* 30**,** 300-315.

[5] DHAWAN, S., SINGLA, A. K. & SINHA, V. R. 2004. Evaluation of Mucoadhesive Properties of Chitosan Microspheres Prepared by Different Methods. *AAPS PharmSciTech,* 5**,** 1-7.

[6] DUBEY, R. R. & PARIKH, R. H. 2004. Two-Stage Optimization Process for Formulation of Chitosan Microspheres. *AAPS PharmSciTech,* 5**,** 1-9.

[7] GAO, J.-G., ZHANG, Y., YU, Y.-F., HAN, Y.-C., ZHANG, B.-Z. & GAO, C.-H. 2011. Preparation of chitosan microspheres loading of 3,5-dihydroxy-4-<i>i</i>-propylstilbene and in vitro release. *Journal of Polymer Research,* 18**,** 1501-1508.

[8] HUANG, J., FU, X., CHEN, X., LI, Z., HUANG, Y. & LIANG, C. 2021. Promising Therapeutic Targets for Treatment of Rheumatoid Arthritis. *Front Immunol,* 12**,** 686155.

[9] JEYANTHI, R., MEHTA, R. C., THANOO, B. C. & DELUCA, P. P. 1997. Effect of processing parameters on the properties of peptide-containing PLGA microspheres. *J Microencapsul.,* 14**,** 163-174.

[10] JOSE, S., PREMA, M. T., CHACKO, A. J., THOMAS, A. C. & SOUTO, E. B. 2011. Colon specific chitosan microspheres for chronotherapy of chronic stable angina. *Colloids and Surfaces B: Biointerfaces,* 83**,** 277-283.

[11] KIKUCHI, A., KAWABUCHI, M., SUGIHARA, M., SAKURAI, Y. & OKANOA, T. 1999. Pulsed dextran release from calcium-alginate gel beads. *Journal of Controlled Release* 47**,** 21-29.

[12] KIKUCHI, A. & OKANO, T. 2002. Pulsatile drug release control using hydrogels. *Adv. Drug Deliv. Rev.,* 54**,** 53-77.

[13] LIU, F., LIU, L., XUEMIN, L. & ZHANG, Q. 2007. Preparation of chitosan-hyaluronate double-walled microspheres by emulsification-coacervation method. *J Mater Sci: Mater Med,* 18**,** 2215-2224.

[14] LORENZO-LAMOSA, M. L., REMUN˜A´N-LO´PEZ, C., VILA-JATO, J. L. & ALONSO, M. L. 1998. Design of microencapsulated chitosan microspheres for colonic drug delivery. *Journal of Controlled Release,* 52**,** 109-118.
[15] MCINNES, I. B. & SCHETT, G. 2011. The pathogenesis of rheumatoid arthritis. *N Engl J Med,* 365**,** 2205-19.
[16] NGIAN, G. S. 2010. Rheumatoid arthritis. *Aust Fam Physician,* 39**,** 626-8.
[17] PACHUAU, L. & MAZUMDER, B. 2009. A study on the effects of different surfactants on thylcellulose microspheres. *International Journal of PharmTech Research,* 1**,** 966-971.
[18] PATEL, G. C. & PATEL, M. M. 2009. A comparative in vitro evaluation of enteropolymers for pulsatile drug delivery system. *Acta Pharmaceutica Sciencia,* 51**,** 243- 250.
[19] PENA, M. 1990. Etodolac: analgesic effects in musculoskeletal and postoperative pain. *Rheumatol Int,* 10 Suppl**,** 9-16.
[20] RADU, A. F. & BUNGAU, S. G. 2021. Management of Rheumatoid Arthritis: An Overview. *Cells,* 10.
[21] ROY, P. & SHAHIWALA, A. 2009. Statistical optimization of ranitidine HCl floating pulsatile delivery system for chronotherapy of nocturnal acid breakthrough. *European Journal of Pharmaceutical Sciences,* 37**,** 363-369.
[22] ROY, S., PANPALIA, S. G., NANDY, B. C., RAI, V. K., TYAGI, L. K., DEY, S. & MEENA, K. C. 2009. Effect of Method of Preparation on Chiosan Microspheres of Mefenamic Acid. *International Journal of Pharmaceutical Sciences and Drug Research,* 1**,** 36-42.
[23] SHIVAKUMAR, H. N., SURESH, S. & DESAI, B. G. 2010. Design and Evaluation of controlled Onset Extended Release Multiparticulate Systems for Chronotherpeutic Delivery of Ketoprofen. *J Mater Sci: Mater Med,* 21**,** 2691-2699.
[24] SHUKLA, P. G., KALIDHASS, B., SHAH, A. & PALASHKAR, D. V. 2002. Preparation and characterization of microcapsules of water soluble pesticide monocrotophs using polyurethane as carrier material. *J Microencapsul.,* 19**,** 293-304.
[25] SMOLEN, J. S., ALETAHA, D. & MCINNES, I. B. 2016. Rheumatoid arthritis. *Lancet,* 388**,** 2023-2038.
[26] SMOLENSKY, M. H., LEMMER, B. & REINBERG, A. E. 2007. Chronobiology and chronotherapy of allergic rhinitis and bronchial asthma. *Adv. Drug Deliv. Rev.,* 59**,** 852-882.
[27] SONI, M. L., NAMDEO, K. P., JAIN, S. K., GUPTA, M., DANGI, J. S., KUMAR, M. & DANGI, Y. S. 2011. pH-Enzyme Di-dependent Chronotherapeutic Drug Delivery System of Theophylline for Nocturnal Asthma. *Chem.Pharm.Bull.,* 59**,** 191-195.
[28] UMADEVI, S. K., THIRUGANESHA, R., SURESHA, S. & REDDYA, K. B. 2010. Formulation and Evaluation of Chitosan Microspheres of Aceclofenac for Colon-Targeted Drug Delivery. *Biopharm. Drug Dispos.,* 31**,** 407-427.
[29] WARWICK, M. T. 1988. Epidemiology of nocturnal asthma. *Am. J. Med.,* 58**,** 6-8.
[30] WASSERMAN, A. M. 2011. Diagnosis and management of rheumatoid arthritis. *Am Fam Physician,* 84**,** 1245-52.
[31] WILDING, R., DAVIS, S. S., POZZI, F., FURLANI, P. & GAZZANIGA, A. 1994. Enteric coated timed release system for colonic targeting. *Int. J. Pharm,* 111**,** 99-102.
[32] ZVAIFLER, N. 1989. A review of the antiarthritic efficacy and safety of etodolac. *Clin Rheumatol,* 8 Suppl 1**,** 43-53.